reported value of 2.97 Mev. A lower-energy component with a relative abundance of 1.5 percent has its upper energy limit at 0.92 Mev. No strong evidence appeared for the existence of a beta ray at an intermediate energy, as previously reported.[3]

The energies of certain gamma rays are observed to be equivalent to the sum of others, suggesting cross-over transitions. It is possible to postulate a reasonable nuclear level scheme for Pr^{144}, as shown in Fig. 3, which satisfies most of the observed data. The intensity relations as well as the coincidence data are about as would be expected from the level scheme.

PHYSICAL REVIEW VOLUME 96, NUMBER 5 DECEMBER 1, 1954

Slow Neutron Cross Sections of Gold, Silver, Indium, Nickel, and Nickel Oxide

R. G. ALLEN,* T. E. STEPHENSON, C. P. STANFORD, AND SEYMOUR BERNSTEIN
Oak Ridge National Laboratory, Oak Ridge, Tennessee

(Received March 1, 1954)

The total reflection and selective attenuation properties of mirrors for neutrons were used to obtain essentially higher order free reflections of a beam of reactor neutrons from a quartz crystal. An arrangement of mirror, crystal, and sample, in series was used to measure the total cross section of Au, Ag, In, Ni, and NiO as a function of neutron wave length over intervals in the region between 0.7A and 4.6A. The results on the strong absorbers Au, Ag, and In were analyzed into absorption and scattering contributions. The absorbers exhibited essentially the $1/v$ characteristic expected. The scattering and absorption cross sections of Au, Ag, and In are compared with previously reported values. For the strong scatterers Ni and NiO, the total scattering, ordered scattering, and disordered scattering cross sections, and the Debye temperature were derived from the energy dependence of the total cross section. The ordered scattering cross section per Ni nucleus was found to be 13.1 ± 0.3 barns. The capture and ordered elastic contributions were subtracted from the experimental curve of total cross section *vs* energy. This residual scattering function of energy was compared to that theoretically expected from a Debye independent-oscillator model and the one-phonon incoherent scattering approximation of Kleinman. In the case of Ni, at the longer wavelengths, both models fit the data well, and at the shorter wavelengths, where multiple phonon processes occur, the independent oscillator model continues to fit the data. For NiO, measurements fit the independent oscillator model at the shorter wavelengths, and lie above the values calculated from either model at the longer wavelengths. Additional measurements of the total cross section of NiO as a function of temperature would be needed to attribute the difference between measured and calculated values at the longer wavelengths definitely to inelastic scattering processes.

I. INTRODUCTION

THE development of high-intensity neutron sources, such as chain reactors, and the utilization of the wave properties of neutrons for diffraction from single crystals provide a relatively simple instrument, the neutron spectrometer, for obtaining nearly monoenergetic neutron beams of usable intensities. The intensity distribution in the neutron spectrum from slow neutron chain reactors is such that, for most commonly used crystals, higher order reflections from the crystal must be considered in certain regions of the spectrum. Bragg's law $n\lambda=2d\sin\theta$ states that for a fixed angle of incidence, wavelengths λ, $\lambda/2$, $\lambda/3$, $\cdots$, having energies E, $4E$, $9E$, $\cdots$, will be present in the beam reflected from a crystal. Since the energy spectrum from a chain reactor is approximately Maxwellian, the presence of the higher orders may not be troublesome at glancing angles corresponding to first order energies E greater than the most probable energy, because the neutron flux decreases rapidly with increasing energy. For energies less than the most probable energy, the presence of higher orders can be very troublesome. The higher order crystal reflections can be removed by use of the total reflection properties of mirrors. (We find that a mirror was used briefly for this purpose in 1945 by L. B. Borst and associates.[1])

The reflectivity of a plane mirror for neutrons of wavlength λ is given by

$$R=\left\{\frac{1-[1-(\lambda/\lambda_f)^2]^{\frac{1}{2}}}{1+[1-(\lambda/\lambda_f)^2]^{\frac{1}{2}}}\right\}^2, \tag{1}$$

where λ_f, the cut-off or critical wavelength is related to the glancing angle of incidence on the mirror, α, by the expression:

$$\lambda_f=\frac{\alpha}{(N\bar{f}/\pi)^{\frac{1}{2}}}. \tag{2}$$

Here, N is the number of nuclei per cm^3 of the mirror material and $\bar{f}$ is the average ordered (coherent) scattering amplitude, due regard being taken of the signs of the individual scattering amplitudes. For a fixed angle of incidence, wavelengths greater than the cut-off wavelength will be totally reflected, whereas the inten-

* Present address: Airforce Special Projects Office, P. O. Box E, Oak Ridge, Tennessee. This work was done at Oak Ridge National Laboratory in partial fulfillment of the requirements for the Ph.D. degree at the University of Texas, while the author was on active duty with the United States Air Force. This arrangement was made through the cooperation of the Oak Ridge Institute of Nuclear Studies.

[1] Borst, Ulrich, Osborne, and Hasbrouck, Atomic Energy Commission Report MDDC 15 (unpublished).

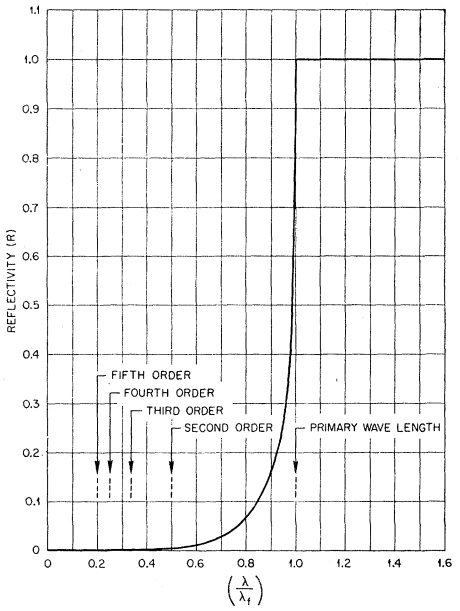

FIG. 1. Reflectivity of a mirror for neutrons incident at a fixed angle of incidence.

sities at wavelengths less than the cut-off wavelength will be attenuated. Equations (1) and (2) apply rigorously when absorption by the mirror is zero, but they are sufficiently accurate for most purposes when the average absorption cross section per atom is less than about 10^4 barns.[2]

Figure 1 gives the reflectivity as a function of λ/λ_f for the case of a perfectly collimated neutron beam. It shows the attenuation of the higher orders when the primary wavelength is taken as λ_f. In practice, the proper choice of mirror angle for acceptable elimination of the higher orders will be influenced by the intensity distribution of the incident spectrum. Figure 2 shows the counting rate obtained from the series arrangement of mirror and quartz crystal of Fig. 3, as a function of wavelength for several mirror angles of incidence α, using as the neutron source the approximately Maxwellian energy spectrum of the Oak Ridge Graphite Reactor. The curves of Fig. 2 can be used to select the proper mirror angle for a desired upper limit to the amount of higher order content in the beam reflected by the crystal.

II. DESCRIPTION OF APPARATUS

Figure 3 shows a schematic diagram of the arrangement of the spectrometer and mirror used for neutron cross section measurements in the wavelength region from 0.7 to 4.6A. In this arrangement, the beam is first collimated by a slit system in the reactor shield. The collimated beam strikes the mirror at a very small glancing angle, is reflected and passes through another slit before reaching the crystal. The beam from the crystal then passes through the sample and into the detector. The collimating slit system in the reactor limits the horizontal beam divergence to approximately ten minutes of arc. The slit adjacent to the crystal is used for further collimation and also to shield the crystal from any portion of the direct beam that was not reflected from the mirror. The additional collimation introduced by the slit at the crystal was variable depending upon the mirror angle and the beam intensity. The mirror consists of four Pyrex glass blocks, each 11.5 in. long by 3.75 in. high by 2 in. thick with the reflecting surfaces polished to optical flatness. These four Pyrex blocks were adjusted as accurately as possible to place the polished surfaces in the same plane. The mirror assembly is equipped with adjustments for positioning it in the beam and for varying the angle between the neutron beam and the mirror.

The spectrometer was an x-ray spectrometer modified to support the heavy paraffin shield surrounding the BF_3 detector tube. Angular settings were reproducible to within 0.5 to 1.0 min of arc. The entire spectrometer was mounted on ways so the crystal could be placed in the beam reflected at different mirror angles. The crystal used with the spectrometer was quartz, oriented to give reflections from the (100) planes. Neutron detection was accomplished with a $B^{10}F_3$ enriched proportional counter and a small $B^{10}F_3$ tube, located at the end of the mirror, served to monitor the beam. Because of the length of time required to obtain the data with the desired accuracy, features were incorporated into the equipment which allowed it to collect and record the required data automatically.

III. CRYSTALLINE SCATTERING OF NEUTRONS

The scattering of neutrons from polycrystalline material, as a function of neutron energy, may be described qualitatively as follows: For neutron energies large compared to the energy binding the atoms in the lattice, the scattering takes place from nuclei that are effectively free. In this case, the collisions are predominantly "inelastic," energy being exchanged with the individual nuclei in dislocating them from their

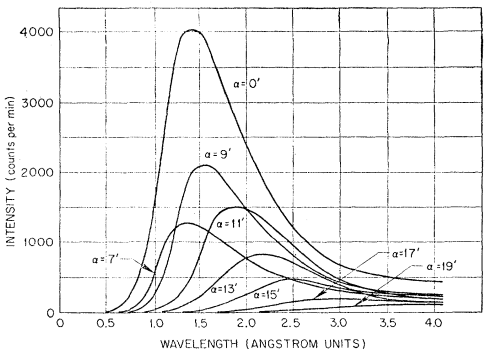

FIG. 2. Intensity reflected from series arrangement of mirror and quartz crystal as a function of neutron wavelength for various mirror angles (α).

[2] M. L. Goldberger and F. Seitz, Phys. Rev. **71**, 294 (1947).

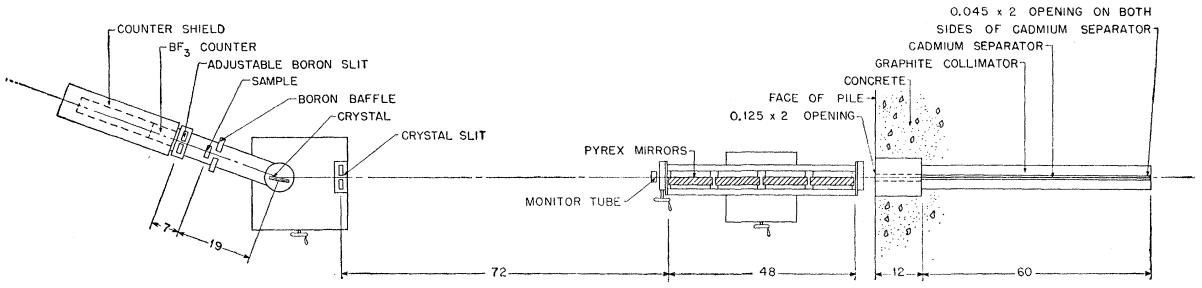

FIG. 3. Schematic diagram of the arrangement of the apparatus.

positions in the lattice. For neutron energies of the order of the crystal binding energy, the collisions are still predominately inelastic, but at these energies, the energy exchange occurs between the neutrons and the lattice as a whole through processes involving the emission or absorption of several sound quanta in the excitation or extinction of elastic vibrations of the crystal lattice. As the energy of the incident neutron decreases, the elastic scattering increases and inelastic scattering processes involving only single phonons predominate. In this energy region, the scattering is characterized by interference effects arising from coherent scattering by the crystal planes. These effects become quite appreciable for materials possessing large ordered (coherent) nuclear scattering cross sections and relatively small capture cross sections. For energies such that the neutron wavelength is greater than twice the maximum plane spacing for which crystal reflections are possible, the ordered elastic or Bragg scattering disappears. Finally, for sufficiently low energies, the incident neutrons have insufficient energy to excite crystal vibrations, but inelastic scattering is still present as a result of the absorption of phonons by the neutrons.

An expression for the total scattering cross section for slow neutrons can be obtained in a rather simple manner following the method used for x-rays[3] where the change in energy upon scattering is assumed negligible in comparison to the incident energy. In the case of neutrons, the effects of isotopes and nuclear spins must be included. In this approximation, a crystal composed of independent oscillators having the same average energy is assumed. Such a model is admittedly a crude approximation since the coupling between atoms is neglected. However, the results obtained under these assumptions are interesting in that, in the case of nickel and nickel oxide, at least, the predicted values for the total scattering cross section for this model are in close agreement with our measured values in the higher energy region where expressions which are limited to single phonon processes do not adequately represent the total inelastic scattering.

On the basis of this "independent oscillator" model the total nuclear scattering cross section per molecule may be written as follows:

$$\sigma_{\text{scattering}}=\sum_a n_a s_a+\sum_a n_a S_a\left[1-\frac{\lambda^2}{P}[1-\exp(-P/\lambda^2)]\right]+\frac{N\lambda^2}{2}\sum_{\tau<2/\lambda}\frac{j_\tau}{\tau}|F_\tau|^2\exp(-\tfrac{1}{4}P\tau^2). \quad (3)$$

In this expression,

$$P=\frac{12h^2}{\bar{M}k_0\Theta}\left[\frac{\phi(x)}{x}+\frac{1}{4}\right], \quad (4)$$

$$\phi(x)=\frac{1}{x}\int_0^x\frac{\beta d\beta}{e^\beta-1}, \quad (5)$$

$$x=\Theta/T, \quad (6)$$

$$F_\tau=\frac{1}{n}\sum_j \bar{f}_j\exp(2\pi i[h_1x_j+h_2y_j+h_3z_j]), \quad (7)$$

$$\bar{f}=(S/4\pi)^{\frac{1}{2}}. \quad (8)$$

Here, h is Planck's constant, k_0 is Boltzman's constant, Θ is the Debye or characteristic temperature of the scattering material, T is the absolute temperature of the scattering material, x_j, y_j, and z_j are the coordinates of the jth nucleus in a unit cell in terms of the lattice constants, $\tau=[d(h_1h_2h_3)]^{-1}$ is the reciprocal of the spacing of the planes designated by the Miller indices $h_1h_2h_3$, S and s are respectively the ordered (coherent) and disordered (incoherent) nuclear scattering cross sections,[4] λ is the neutron wavelength, j_τ is the multiplicity of the $h_1h_2h_3$ reflection, n represents the number of molecules per unit cell, N is the number of molecules per unit volume of crystal, n_a is the number of atoms of type a per molecule and $\bar{M}$ is the average atomic mass of the molecule. If the cross section per nucleus is desired, in the case of a substance consisting of only one element, the index a and the summation over this index are neglected and n and N refer to atoms rather than molecules. The τ summation in expression (3) is performed over all values of τ less than $2/\lambda$ and the j

[3] R. W. James, *The Optical Principles of the Diffraction of X-rays* (G. Bell and Sons, Ltd., London, 1948).

[4] J. M. Cassels, *Progress in Nuclear Physics* (Academic Press, Inc., New York, 1950), p. 185.

summation in expression (7) is performed over all atoms in a unit cell.

The first sum in Eq. (3) is simply the disordered or incoherent nuclear cross section, the second sum has been called the thermal diffuse cross section,[5] $E_{td}(S)$, and the last sum is the ordered elastic or Bragg cross section, $E(S)$. At short wavelengths, where many planes contribute to the ordered elastic scattering, the summation over τ, in this term, may be replaced by an integration,[6] with the result:

$$E(S)=\sum_a n_a S_a\{(\lambda^2/P)[1-\exp(-P/\lambda^2)]\}. \quad (9)$$

Thus, at short wavelengths for the independent oscillator approximation, the total nuclear scattering cross section reduces to the constant value

$$\sigma_{\text{scattering}}=\sum_a n_a(s_a+S_a). \quad (10)$$

Weinstock[7] considered the scattering of neutrons from a Debye crystal consisting of a single spinless isotope, taking into consideration only zero phonon and single phonon processes. Cassels[4] extended Weinstock's calculation to include the effects of isotopes and nuclear spins. The use of the explicit expressions deduced by Weinstock and Cassels is laborious. Kleinman[8,9] calculated the total cross section for inelastic scattering from a Debye crystal for one phonon processes by treating the inelastic scattering as incoherent (disordered). This approximation replaces the summation over crystal planes by an integral. Kleinman has tabulated values of the functions involved, so that a numerical computation of a specific total inelastic scattering cross section can be done simply. Finkelstein[10] has calculated the inelastic scattering cross section for an Einstein crystal for collisions in which a single oscillator changes its energy by one or more phonons and an approximate calculation of the inelastic scattering cross section for events in which more than one oscillator simultaneously change their energy by one phonon has been made by Squires[11] for a Debye crystal.

We have calculated the total nuclear scattering cross section as a function of wavelength for Ni and NiO in the region in which our measurements were made using both Kleinman's "incoherent scattering" approximation and the independent-oscillator model for the nuclear scattering. Since Ni is ferromagnetic and NiO is antiferromagnetic at room temperature, the effects of coherent magnetic scattering were included in the calculated values of the total cross section using the theory of magnetic scattering described by Halpern and Jonhson.[12] For unpolarized neutrons incident upon a polycrystalline magnetic substance, the magnetic and nuclear scattering are independent. The coherent magnetic scattering is calculated on the basis of expressions similar to the ordered elastic term of Eq. (3), taking into consideration the known chemical and magnetic structure of these substances,[13] and the magnetic scattering amplitudes[14] as a function of scattering angle.

IV. EXPERIMENTAL RESULTS AND THEIR INTERPRETATION

The total cross section for neutrons is a measure of the loss of neutrons from the incident beam due to all causes, including absorption and scattering, and is expressed through the relation

$$\sigma_{\text{total}}=-(1/Nt)\ln T, \quad (11)$$

in which N is the number of interacting centers per cm^3, and t is the thickness of the scatterer in cm. T is the sample transmission, the ratio of the transmitted intensity, I, to the incident intensity, I_0.

Neutron cross section measurements were made for various materials in the energy region 0.17 to 0.0038 ev, corresponding to wavelengths 0.7 to 4.6A. These materials can be divided into two groups, absorbers and scatterers. The absorbers were gold, indium, and silver in the form of thin foils and the scatterers were nickel and nickel oxide in the form of very fine powders. Spectrographic analysis of the samples showed negligible amounts of impurities in all samples. Sufficient counts were collected for the measured values of the cross sections so that their statistical probable errors are, in most cases, less than about 1 percent.

A. Absorbers

Figure 4 shows the measured values for the total cross section of gold made with and without the mirror. The falling off, with increasing wavelength, of the curve obtained without the mirror shows clearly the effect of

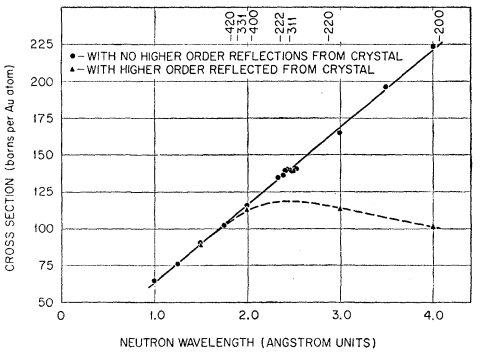

FIG. 4. Total cross section of gold as a function of neutron wavelength measured with and without mirror, showing effectiveness of the mirror in elimination of higher order reflections from crystal.

[5] E. O. Wollan and C. G. Shull, Phys. Rev. **73**, 830 (1948).
[6] Halpern, Hamermesh, and Johnson, Phys. Rev. **59**, 981 (1941).
[7] R. Weinstock, Phys. Rev. **65**, 1 (1944).
[8] D. A. Kleinman, dissertation, Brown University, 1951 (unpublished).
[9] D. A. Kleinman, Phys. Rev. **81**, 326 (A) (1951).
[10] R. J. Finkelstein, Phys. Rev. **72**, 907 (1947).
[11] G. L. Squires, Proc. Roy. Soc. (London) **A212**, 192 (1952).
[12] O. Halpern and M. H. Johnson, Phys. Rev. **55**, 898 (1939).
[13] Shull, Strauser, and Wollan, Phys. Rev. **83**, 333 (1951).
[14] Shull, Wollan, and Koehler, Phys. Rev. **84**, 912 (1951).

higher orders on the values obtained for the total cross section if no corrections are made for the presence of the higher order wavelengths. The effectiveness of the mirror in eliminating the higher order reflections can be judged by the fact that, with the mirrors present, the values measured at long wavelengths and the values measured at short wavelengths fall closely along a straight line, as would be required by a $1/v$ relationship.

Figure 5 gives the measured results for the total cross section of gold, indium, and silver as a function of wavelength from about 1A to 4A. In order to consider the effect of the nearest resonance, these data were fitted by least squares to an equation of the form

$$\sigma_t = c_1(\lambda + 2\lambda_0^2/\lambda) + c_2, \tag{12}$$

where λ is the neutron wavelength and λ_0 is the wavelength of the nearest resonance. The values 4.8 ev, 5.1 ev, and 1.45 ev, respectively were used for the nearby resonance levels in Au, Ag, and In. The values of c_1 and c_2 determined by this method are given in Table I along with the value of the capture cross section for neutrons of velocity 2200 meters per second. The term $c_1[\lambda+(2\lambda_0^2/\lambda)]$ represents the absorption cross section, and is obtained as an approximation to the Breit-Wigner one-level resonance formula. Its accuracy depends upon the neutron energy being much less than the resonance energy, and upon $|E-E_0|$ being greater than the total width of the level. For In, Ag, and Au, the expression should be accurate to one or two percent in the interval covered by the data.

In principle, discontinuities in the total cross section should occur at wavelengths satisfying $\lambda=2d(h_1h_2h_3)$ for these materials as expressed by the term for the ordered elastic cross section. However, the ordered elastic cross section for these materials is small compared to the capture cross section and the crystalline effects are difficult to observe. The inset in Fig. 5 shows the measured values for gold in the region of the (311) discontinuity at 2.45A on an expanded scale. The data exhibit the presence of this discontinuity but measurement of the height is impractical. In order to observe this small effect, a discontinuity height of about 2 percent of the total cross section at this wavelength, sufficient data were collected to give a probable error less than 0.7 percent for each cross section value. The inset for Ag covers the region of the (222) discontinuity. It does not show a discontinuity because of the small ordered cross section of Ag.

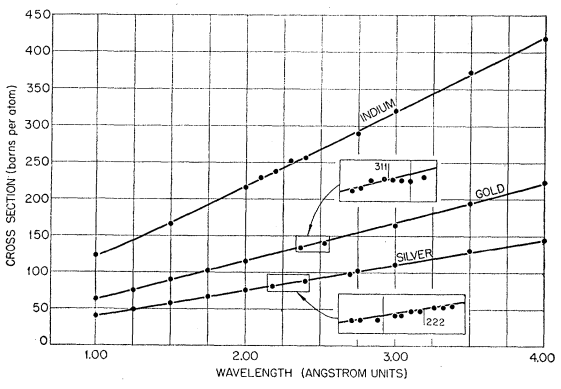

FIG. 5. Total cross section of gold, indium, and silver as a function of neutron wavelength.

TABLE I. Measured constants for absorbers.

Element	c_1 barns/atom angstrom	c_2 scattering barns/atom	σ_a barns/atom (2200 m/sec)	σ_a barns/atom (2200 m/sec)*
Gold	53.1±0.4	8.7±0.9	96.5±0.7	94±1
Silver	35.2±0.3	4.2±0.7	64.0±0.5	60±3
Indium	102.3±1.0	8.6±2.4	190.2±1.8	190±10

* See reference 15.

Our values of the absorption cross sections of Au, Ag, and In at 2200 m/sec agree quite well with the best available estimates of these cross sections as determined by the Atomic Energy Commission Neutron Cross Section Advisory Group,[15] which are given in the last column of Table I. A recent value[16] of 98.7±0.7b for the absorption cross section of Au at 2200 meters per second has been derived from measurements in the region 1.5 to 10A.

B. Scatterers

The samples of nickel and nickel oxide consisted of circular disks pressed from fine powder and placed in sealed aluminum containers having thin windows. The average particle size for each of these powders was estimated to be between one half and one micron from photographs of the particles under a magnification of 2000 diameters. For particles of this size, extinction effects may be considered negligible.[17] The samples were pressed in order to prevent density changes resulting from the frequent movement and inevitable slight jars which they receive in being positioned in the neutron beam. Because of intensity requirements, the samples were fairly large, approximately two inches in diameter. Several sample thicknesses, from about $\frac{1}{8}$ in. to $\frac{1}{2}$ in. were used. Table II gives the physical properties of the various specimens. Efforts were made to prepare the samples from dry material, samples being exposed to the atmosphere only during the time necessary to load the powder into the press. In preparing the nickel oxide sample, the powder was heated to 300°C and maintained at this temperature for four hours in an effort to eliminate any adsorbed water. The powder was then cooled in a dry atmosphere before pressing. Water analyses failed to show detectable amounts of water in the nickel oxide powders. However, it is difficult to

[15] *Neutron Cross Sections*, Atomic Energy Commission Report, AECU-2040 (Technical Information Division, Department of Commerce, Washington, D. C., 1952).

[16] Carter, Palevsky, Myers, and Hughes, Phys. Rev. **92**, 716 (1953).

[17] R. J. Weiss, Phys. Rev. **86**, 271 (1952).

TABLE II. Physical properties of powder samples.

Sample	Thickness (inches)	No. atoms or molecules per cm²	Apparent density (g per cm³)
Nickel No. 1	0.465	7.67×10^{22}	6.33
Nickel No. 2	0.127	2.00×10^{22}	6.06
Nickel oxide No. 1	0.477	3.00×10^{22}	3.07
Nickel oxide No. 2	0.401	3.18×10^{22}	2.62

make accurate chemical analyses for water in samples of this kind. Neutron measurements at low energies will be affected strongly by even small amounts of water. Since a departure from a random orientation of the particles in the powder sample could have a serious effect on the value obtained for the ordered elastic scattering cross section determined by the method of these measurements, a search for departure of the particle orientations from a random distribution was made by measuring the scattered intensity at various points on a Debye ring. Results showed no evidence of a preferred orientation.

1. *Nickel*

Since Ni has a face-centered cubic structure, the crystal structure factor, F_r, becomes for Ni simply $\bar{f}_{\mathrm{Ni}}$ for all Miller indices odd or all indices even, and becomes zero for any combination of odd and even indices. Discontinuities in the cross section will occur at values of λ satisfying $\lambda=2d(h_1h_2h_3)$, where $d(h_1h_2h_3)$ may be written as a_0/L with $L=(h_1^2+h_2^2+h_3^2)^{\frac{1}{2}}$ and $a_0=3.517$A. From Eq. (3) an expression for the height of the discontinuity, H_L, for a particular value of L may be written in the form:

$$\frac{H_L}{(8j_L/L^3)}=|\bar{f}|^2\exp[-A\Phi(x)L^2]. \tag{13}$$

Here,

$$A=\frac{3h^2}{Mk_0Ta_0^2},\quad \Phi(x)=\frac{1}{x}\left[\frac{\phi(x)}{x}+\frac{1}{4}\right].$$

Equation (13) represents a linear relationship between $\ln(H_LL^3/8j_L)$ and L^2. The slope of this line is a known function of Θ, and its intercept with the axis of ordinates at $L^2=0$ is equal to $\ln|\bar{f}|^2$. Such a plot, using the measured discontinuity heights, is exhibited in Fig. 6 with the straight line shown determined from the data

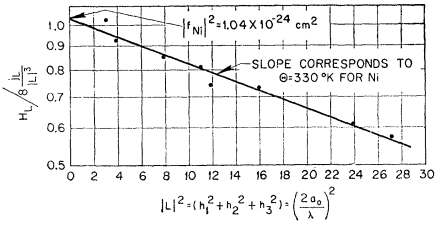

FIG. 6. Determination of the ordered scattering amplitude and Debye temperature for nickel.

by the procedure of least squares. The values obtained for the ordered scattering cross section per nickel nucleus and the Debye temperature are: $S=13.1\pm0.3$ barns/atom; $\Theta=330$°K. Table III gives the measured heights and compares them with those calculated from Eq. (13) using the experimentally determined values of S and Θ. Our value of 13.1 ± 0.3 barns compares very well with the value 13.4 barns obtained from powder diffraction patterns.[18] The value of this quantity has special practical significance since it is generally used as a secondary standard in neutron diffraction work. The value, 13.4 barns, was determined by comparison of the intensity of scattering from a normal nickel sample to the intensities scattered from a set of calibrated scatterers,[18] one of which was diamond dust. An independent absolute measurement of $\bar{f}$ for nickel, such as that obtained from these measurements, confirms the absolute measurement on diamond and the nickel-carbon comparison. Our value for the Debye temperature may be compared with the value 370°K, obtained from neutron diffraction measurements[19] and the values

TABLE III. Nickel discontinuity heights.

Plane $(h_1h_2h_3)$	L^2	Wavelength A^0	Calculated height, barns/atom	Measured height, barns/atom
111	3	4.06	12.0	12.7
200	4	3.52	5.7	5.5
220	8	2.49	3.7	3.6
311	11	2.12	4.3	4.3
222	12	2.03	1.2	1.2
400	16	1.76	0.5	0.6
331	19	1.61	1.6	···
420	20	1.57	1.4	···
422	24	1.44	1.0	1.0
333, 511	27	1.35	1.0	1.1

400°K and 413°K, determined by specific heat measurements.[20]

The cross section at wavelengths greater than the Bragg cutoff, 4.016A for nickel, should be due entirely to capture, inelastic scattering and disordered scattering resulting from the presence of isotopes. There is negligible disordered scattering due to nuclear spins, since normal nickel may be considered as composed essentially of spinless isotopes. A first estimate of the disordered cross section per nucleus may be obtained from measurements in the wavelength region beyond the Bragg cutoff. Taking the capture cross section of nickel as 4.5 barns at 0.025 ev,[21] and assuming a $1/v$ relation, the capture cross section may be computed for the region beyond the Bragg cutoff. The thermal diffuse cross section can be calculated from the second term in Eq. (3), since this quantity depends upon S and Θ. Subtraction of the capture and thermal diffuse cross

[18] C. G. Shull and E. O. Wollan, Phys. Rev. **81**, 527 (1951).
[19] C. G. Shull and E. O. Wollan (unpublished).
[20] M. W. Zemansky, *Heat and Thermodynamics* (McGraw-Hill Book Company, Inc., New York, 1950).
[21] H. Pomerance, Phys. Rev. **83**, 641 (1951).

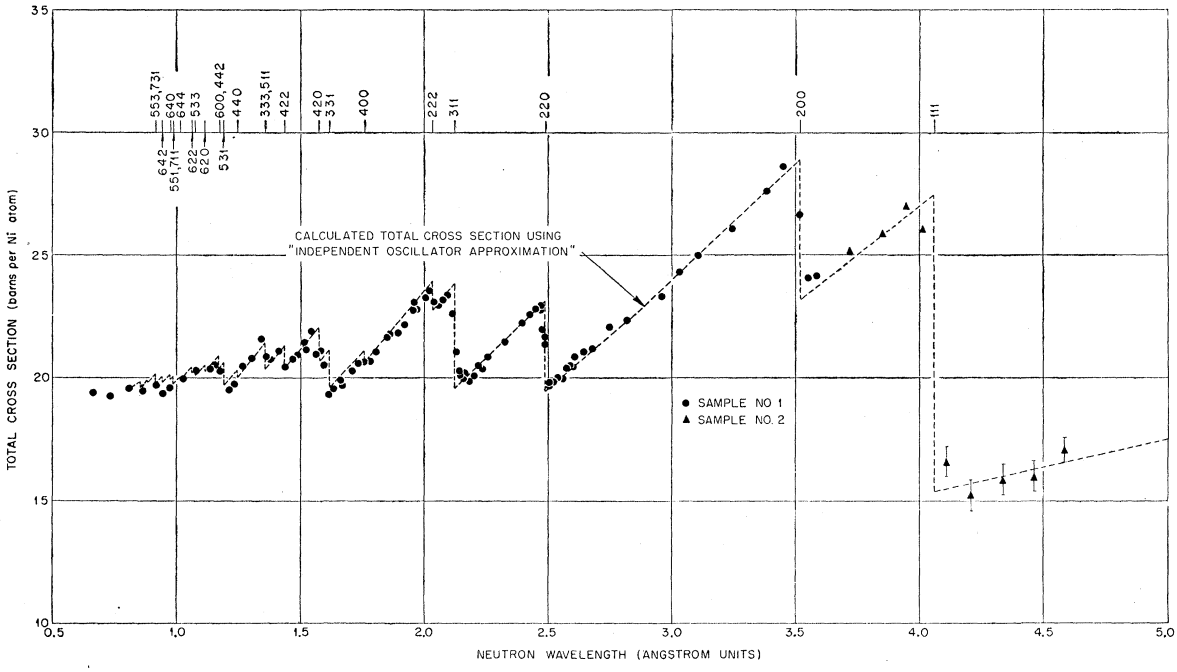

FIG. 7. Total cross section of nickel as a function of neutron wavelength.

sections from the measured values in this region leaves only the disordered scattering cross section. The value of s obtained in this manner should be in accord with the value obtained by an extrapolation of the total cross section to $\lambda=0$ which gives $\sigma_{\text{scattering}}=S+s$. Finally, the values of S and s should be consistent with the measured total cross section over the entire range of measurements. From these considerations the value of s which best fits the data was found to be 4.8 barns.

Figure 7 shows the measured total cross section as a function of wavelength compared to the values for the total cross section calculated on the basis of the independent oscillator model, using the values of S, s, and Θ derived from our data. The capture and ordered elastic contributions were subtracted from the experimental values of the total cross section *vs* energy. Since the quantities subtracted from the measured values are the same for either the independent oscillator approximation or the incoherent approximation, the residual experimental function of energy, represented by the points of Fig. 8, was compared to the scattering function of energy expected from each of these approximations. The incoherent approximation fits the data only at the longer wavelengths, as is to be expected from a one phonon theory. The independent oscillator approximation fits the data over the entire region of observation on the basis of values for S, s, and Θ derived entirely from these measurements alone. This agreement with the independent oscillator approximation is interesting in that this simple approximation seems to account for the total scattering, for Ni, over this range of measurements, and for NiO at the short wavelengths. At longer wavelengths, i.e., beyond the Bragg cut off, the independent oscillator approximation fails to predict the linear increase in scattering cross section with wavelength that is predicted by the more rigorous approach and which is experimentally observed. From these measurements, the total inelastic scattering cross section, $e(s,S)$, can be represented semi-empirically by an expression of the form

$$e(s,S)=(s+S)\{1-(\lambda^2/P)[1-\exp(-P/\lambda^2)]\}, \quad (14)$$

which agrees with the generally accepted conclusion that the sum of the elastic and inelastic nuclear scattering is constant for the shorter wavelengths.

The ferromagnetic scattering of the powdered Ni sample was calculated for $\lambda=2d(111)$ where the magnetic scattering is greatest, and found to be only 0.15 barn, or about one percent of the (111) discontinuity height due to nuclear scattering. Consequently the effects of magnetic scattering for Ni were considered

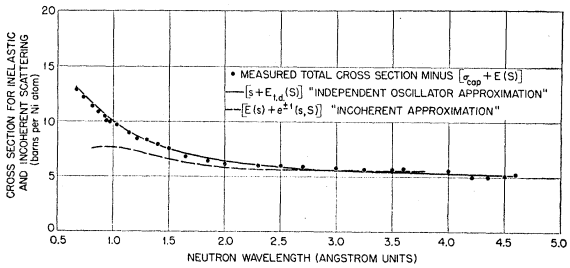

FIG. 8. Inelastic plus disordered cross section of nickel as a function of neutron wavelength.

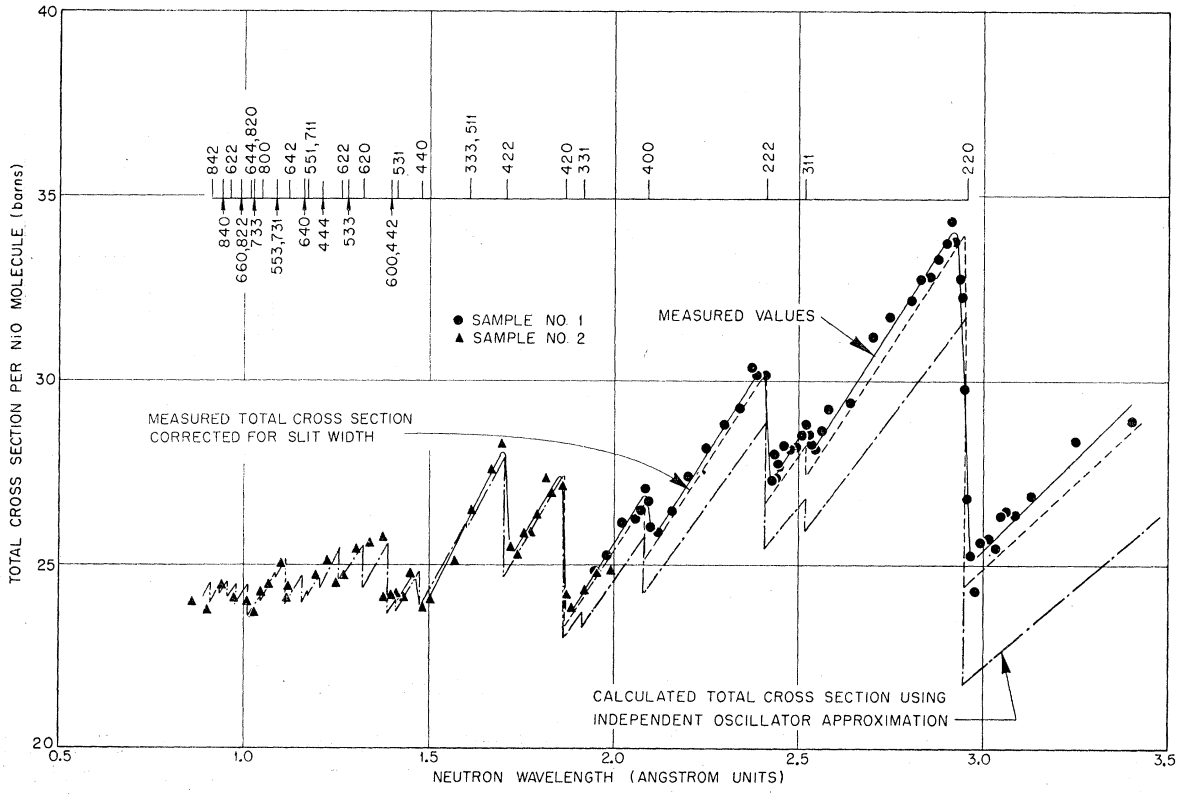

FIG. 9. Total cross section of nickel oxide as a function of neutron wavelength.

negligible. In these calculations the magnetic form factor for Ni was approximated by that for iron.[22]

2. *Nickel oxide*

Measurements were made with a nickel oxide sample in the same fashion as those described for nickel. At room temperature nickel oxide is a face centered cubic with NaCl structure. The crystal structure factor per molecule was taken as $(\bar{f}_{Ni} \pm \bar{f}_0) \exp(-\frac{1}{4}P\tau^2)$, where the positive sign applies to all indices even, the negative sign to all indices odd. The structure factor is zero for any combination of odd and even indices. Taking the spins of the nickel and oxygen isotopes as zero, and treating oxygen as essentially mono-isotopic, the disordered cross section may be taken simply as that due to the isotopes in nickel, i.e., 4.8 barns. Employing the same methods used for nickel, the quantity $|\bar{f}_{Ni}+\bar{f}_0|^2$ and Θ can be determined from the measured heights of the discontinuities resulting from planes characterized by even Miller indices. In principle, $|\bar{f}_{Ni}-\bar{f}_0|^2$ and Θ could be determined from the odd reflections. Since the discontinuities resulting from these planes are much smaller than those from the even planes, such a procedure is impractical. Using 4.2 barns[18] for the ordered scattering cross section, S_O, of oxygen, the value obtained for S_{Ni} was 13.2 barns, and the measured Debye characteristic temperature was 495°K. Using the height of the (311) discontinuity, both S_{Ni} and S_O can be found. This procedure gives $S_{Ni}=13.4$ barns and $S_O=4.1$ barns. This method uses only one odd discontinuity height, however, and it is felt that the value of 13.2 barns represents the better measurement in the case of NiO. The calculated discontinuity heights for nickel oxide are compared with the measured values in Table IV.

TABLE IV. Nickel oxide discontinuity heights.

Plane $(h_1h_2h_3)$	L^2	Wavelength A	Calculated height, barns/molecule	Measured height, barns/molecule
111	3	4.82	2.3	···
200	4	4.17	14.7	···
220	8	2.95	9.9	9.8
311	11	2.52	0.9	1.0
222	12	2.41	3.4	3.5
400	16	2.09	1.6	1.6
331	19	1.91	0.4	···
420	20	1.87	4.4	4.2
422	24	1.70	3.2	3.2

In Fig. 9, the points represent the values of the total cross section deduced from the actually measured values of the sample transmission. The solid curve is drawn through these points. The NiO data were the first to be taken. After it had been taken, it was found that the detector window had not been quite wide

[22] J. Steinberger and G. C. Wick, Phys. Rev. **76**, 994 (1949).

enough to accept all small angle scattered neutrons. The necessary corrections to the solid curve were determined by studying the effective cross section at 3.4A as a function of detector slit width. The solid curve value at 3.4A had to be reduced by 3 percent, or 0.75b. Corrections at other wavelengths were made by assuming that the necessary correction for small angle scattering was zero at 1.6A and less, and that it increased linearly with wavelength. The dashed curve of Fig. 9 represents the total cross section which would have been measured if the detector slit had accepted all small angle scattered neutrons. The dot-dash curve is the calculated total cross section. It includes capture, ordered elastic scattering, disordered scattering due to Ni isotopes, thermal diffuse scattering on the independent oscillator model, and magnetic scattering. The ordered magnetic scattering was computed following the methods previously mentioned[13] with the magnetic form factor of the Ni ion approximated by that for Mn ion. The magnetic contribution to the total scattering is appreciable, about 0.9b at $\lambda=3.4$A. The experimental and calculated curves agree well at the short wavelengths, but disagree quite markedly at the longer wavelengths.

The good agreement between the calculated and observed ordered elastic scattered effects in Ni alone, and in NiO alone, and the agreement between the values of S from the Ni data and the NiO data, suggest that the difference between calculated and observed total cross section of NiO of Fig. 9 can not be attributed to ordered elastic scattering. It seems unlikely that it is due to the use of an incorrect value for the capture cross section. The presence of water in the sample does not seem a likely candidate to account for the difference between the observed and calculated values, since great care was taken to remove the water. Furthermore, if one assumes the sample to have contained an amount of water sufficient to give agreement between calculated and observed values at some one energy, the agreement fails to persist at other wavelengths.

In Fig. 10, the plotted points represent the measured total cross section values minus the contributions from capture, coherent nuclear and coherent magnetic scattering as a function of wavelength. The solid curve

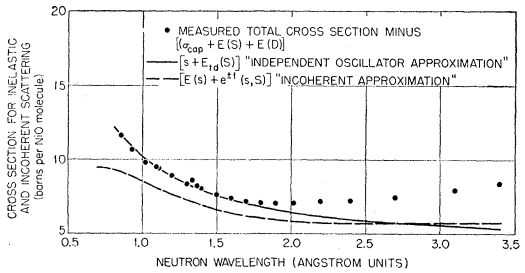

FIG. 10. Inelastic plus disordered cross section of nickel oxide as a function of neutron wavelength.

represents the corresponding calculated values using the independent oscillator model and the dashed curve represents the values from the incoherent approximation. This first model agrees with the points at short wavelengths, the second model does not. Neither model fits the data at the long wavelengths. The points lie about 3 barns above the calculated curves at 3.4A. The incoherent approximation should show a minimum due to lattice inelastic scattering at a wavelength greater than that at which the minimum occurs in the data.

Simultaneous one phonon processes, which were not included in the calculated cross section curves, should decrease slightly the difference between the measured and calculated values of Figs. 9 and 10. There is also the possibility that the difference may be due, in part, to magnetic inelastic scattering[23–25] as well as to lattice inelastic scattering. Additional measurements of the cross section of NiO as a function of temperature are needed to relate the difference definitely to inelastic scattering of either or both types. Measurements in the region beyond the Bragg cutoff should also be helpful.

We wish to acknowledge our appreciation to Drs. C. G. Shull, E. O. Wollan, and S. Tamor for helpful discussions on neutron scattering. We are indebted to Miss T. Arnette for help in taking the data, to R. M. Steele for x-ray studies of our samples, and to C. Feldman for spectroscopic analyses of the samples.

[23] R. G. Moorhouse, Proc. Phys. Soc. (London) **A64**, 1097 (1951).
[24] H. Palevsky and D. J. Hughes, Phys. Rev. **92**, 202 (1953).
[25] L. Van Hove (unpublished).